Supporting Information

Microfluidic Immuno-Biochip for Detection of Breast Cancer Biomarkers Using Hierarchical Composite of Porous Graphene and Titanium Dioxide Nanofibers

Md. Azahar Ali[a], Kunal Mondal[b], Yueyi Jiao[a], Seval Oren[a], Zhen Xu[a], Ashutosh Sharma[c], and Liang Dong[a,*]

[a]Department of Electrical and Computer Engineering, Iowa State University, Ames, IA 50011, USA
[b]Department of Chemical and Biomolecular Engineering, North Carolina State University, Raleigh, NC 27695, USA
[c]Department of Chemical Engineering, Indian Institute of Technology Kanpur, Kanpur 208016, India

[*]Corresponding Author: Liang Dong; E-mail: ldong@iastate.edu; Phone: +1-515-294-0388

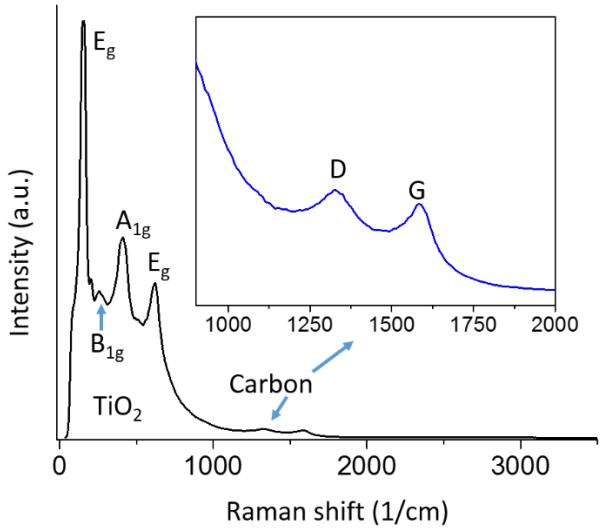

Figure S1. Raman spectra of $nTiO_2$ (calcined at 350 °C) taken at room temperature (25 ºC). Inset shows the carbon signature present in $nTiO_2$.

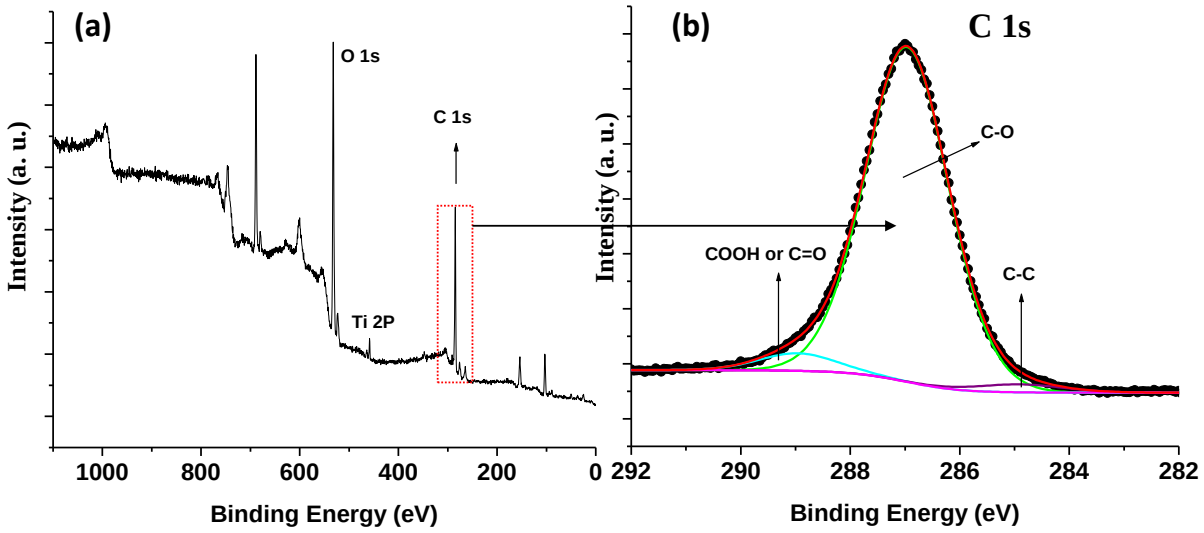

Figure S2. Wide-scan spectra (a) and C 1s spectra (b) for carbon-doped $nTiO_2$.

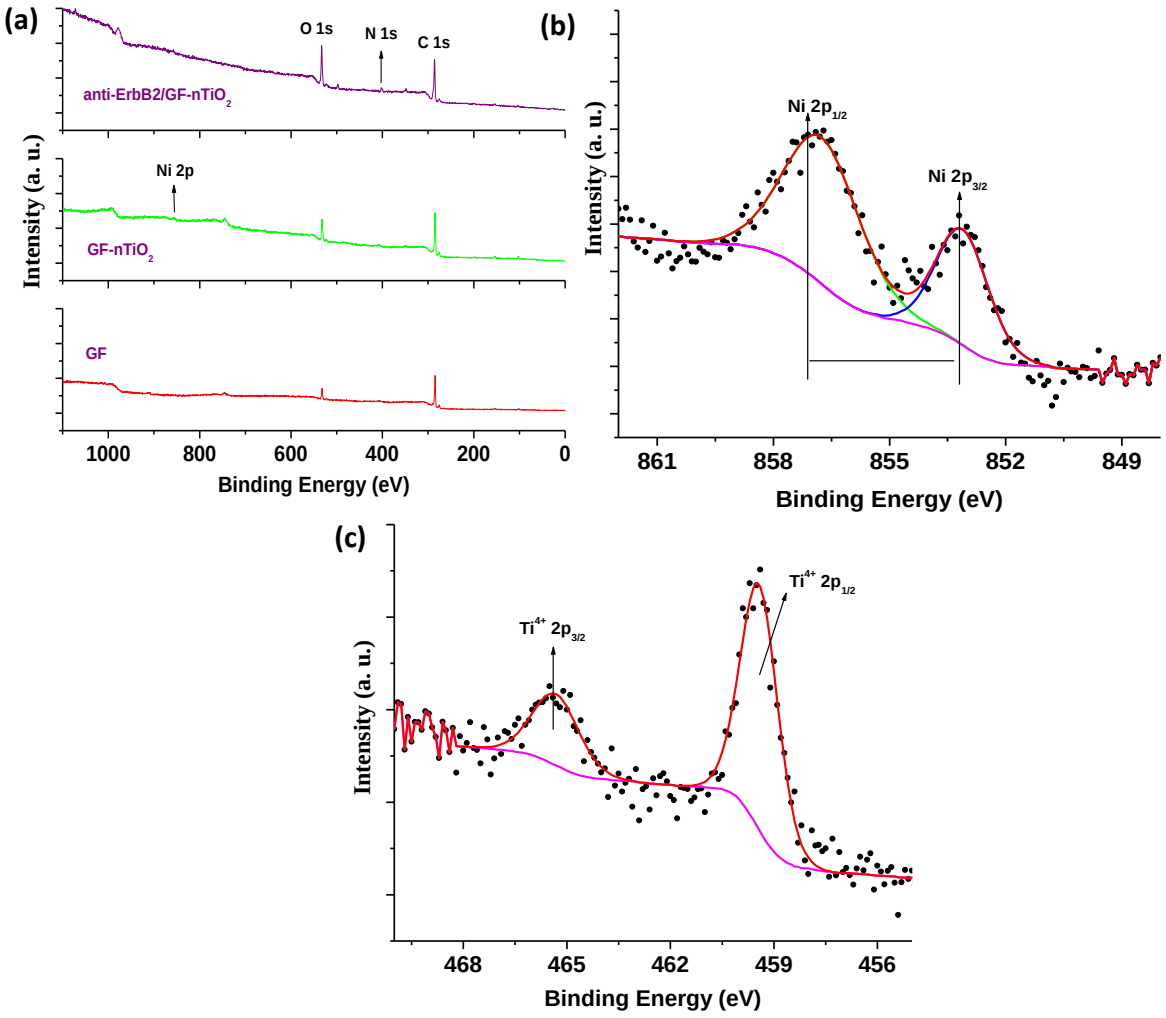

Figure S3. (a) Wide-scan spectra for free-standing GF, GF-nTiO_2 composite, and anti-ErbB2/GF-nTiO_2. (b) Core-level Ni 2p spectra for GF-nTiO_2 composite. (c) Core-level Ti 2p spectra for GF-nTiO_2 composite.

Table S1. Binding energies, full width half maximum (FWHM), and atomic ratio of deconvoluted peaks for C1s, O 1s and N 1s in different samples.

C 1s	**GF (C 1s)**	**B.E. (eV), Atomic (%)**	**FWHM**	**O 1s**	**GF (O 1s)**	**B.E. (eV), Atomic (%)**	**FWHM**	**Ni 2p**	**GF (Ni 2p)**	**B.E. (eV), Atomic (%)**	**FWHM**
	C-C	284.3 (37.6%)	1.26		C=O	532.1 (36.7%)	1.72		Ni $2p_{1/2}$	856.7 eV (64.4%)	2.3
	C=O	285.2 (63.4%)	2.43		C-O	532.6 (58.7)	2.26		Ni $2p_{3/2}$	853.1 eV (35.8%)	1.59
	GF-nTiO_2 (C 1s)	**B.E. (eV), Atomic (%)**	**FWHM**		**GF-nTiO_2 (C 1s) (O 1s)**	**B.E. (eV), Atomic (%)**	**FWHM**	**Ti 2p**	**GF-nTiO_2 Ti 2p**	**B.E. (eV), Atomic (%)**	**FWHM**
	C-C	284.3 (37.1%)	1.26		C-O	532.7 (91.7%)	2.22		Ti 2 $p_{1/2}$	459.4eV (74.4%)	1.26
	C-O	285.2 (56.7%)	2.44								
	O-C=O	288.9 (6.0%)	3.2		C=O	530.33 (8.23%)	1.43		Ti 2 $p_{3/2}$	465.3eV (26.5%)	1.58
	anti-ErbB2/ GF-nTiO_2 (C 1s)	**B.E. (eV), Atomic (%)**	**FWHM**		**anti-ErbB2/ GF-nTiO_2 (O 1s)**	**B.E. (eV), Atomic (%)**	**FWHM**	**N 1s**	**anti-ErbB2/GF-nTiO_2 (N 1s)**	**B.E. (eV), Atomic (%)**	**FWHM**
	C-O	286.3 (35%)	1.76		C-O-C	533.7 (96.5%)	2.5		N1	398.3 (3.5%)	2.25
	N-C=O	287.1 (55.7%)	2.97						N2	401.3 (27.1%)	1.97
	O-C=O	290.0 (9.6%)	1.86		C=O	537.3 3.5%)	1.6		N3	402.7(69.3%)	2.9

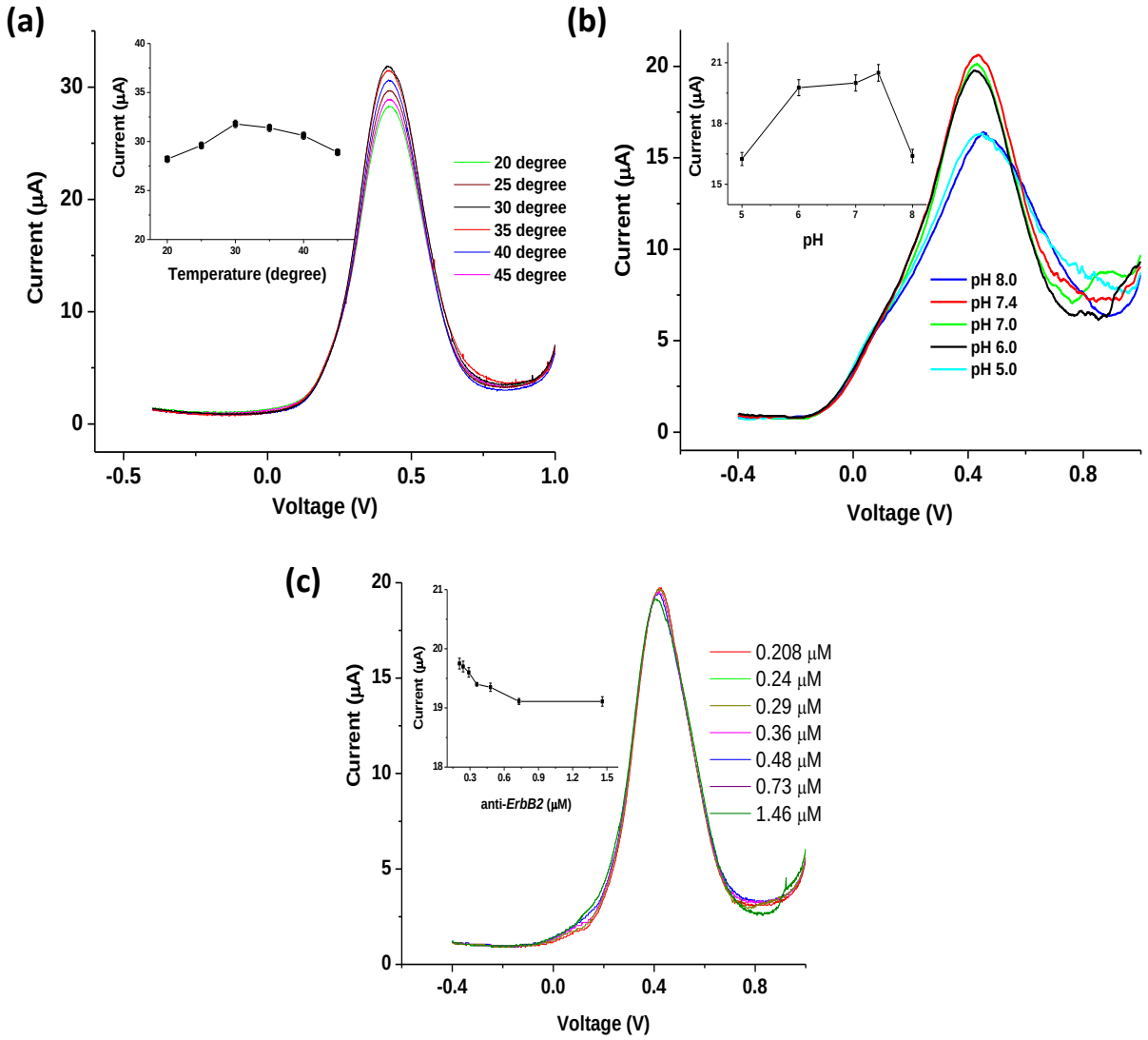

Figure S4. (a) DPV responses of the sensor to 0.1 μM concentration of ErbB2 antigen under different temperatures from 20 ºC to 45 ºC. (b) DPV responses for the sensor to 0.1 μM concentration of ErbB2 antigen in PBS solutions of different pH values. (c) DVP responses of the sensor functionalized with different anti-ErbB2 concentrations when responding to 0.1 μM concentration of ErbB2.

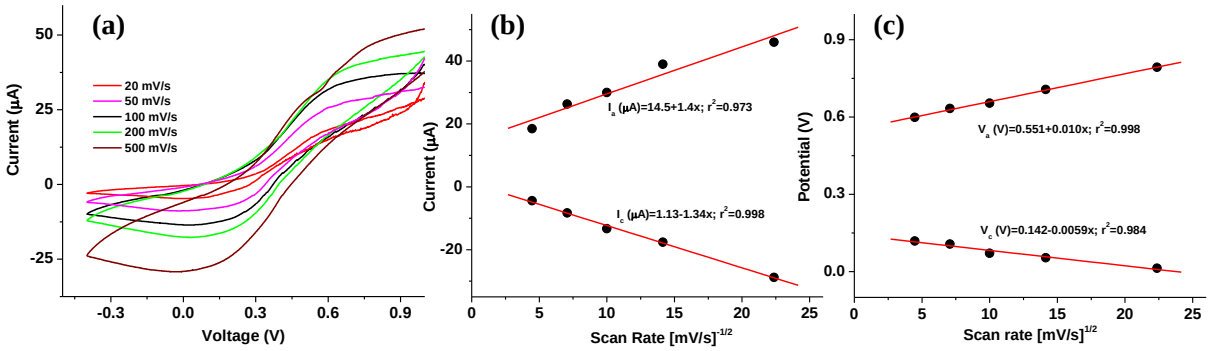

Figure S5. (a) Cyclic voltammetry measurements for the fabricated microfluidic immunochip as a function of scan rate (20-500 mV/s). The experiment was conducted in 50 mM PBS containing 5mM $[Fe(CN)_6]^{3-/4-}$ at pH 7.4. (b) Anodic and cathodic current and (c) potential as a function of root mean square of scan rate. Insets in (b) and (c) show the linear equations with slopes and intercepts values.

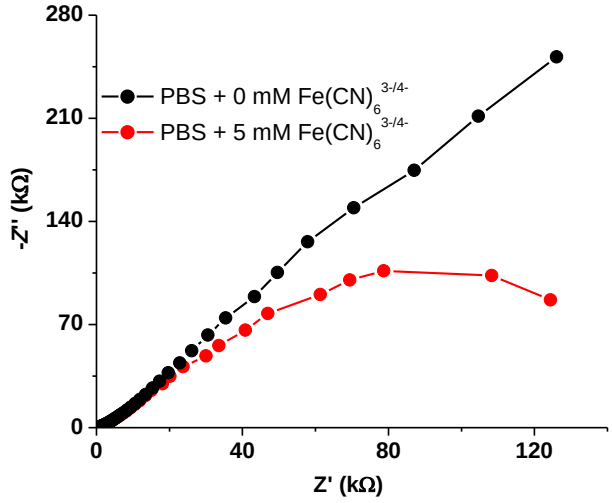

Figure S6. Control studies for the fabricated immunosensor (BSA/anti-ErbB2/GF-TiO_2) with and without $Fe(CN)_6^{3-/4-}$ in PBS solution.

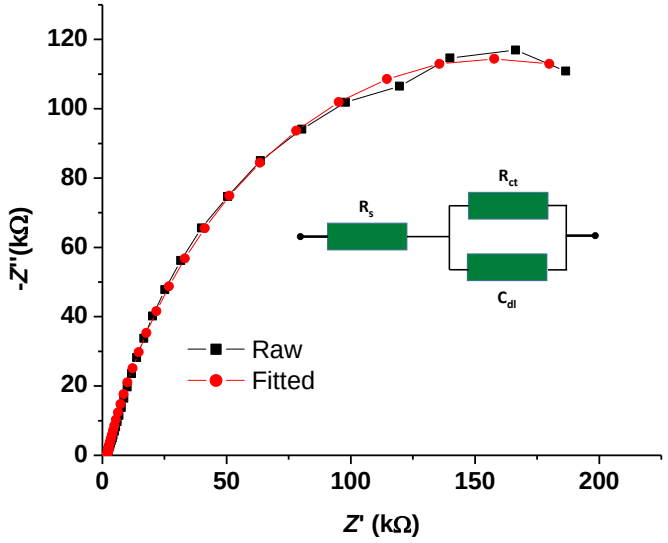

Figure S7. Nyquist plots for raw and fitted data obtained at 10^{-14} M concentration of ErbB2. The inset shows a simplified circuit model for extracting R_{ct} value.

Table S2. Charge transfer resistances, solution resistances and double layer capacitances of the sensor obtained at different concentrations of target ErbB2 antigen.

ErbB2 concentration (M)	Charge transfer resistance R_{ct} (kΩ)	Solution resistance R_s (kΩ)	Double layer capacitance C_{dl} (μF)
0	152 ± 17.56	5.0	6.0
10^{-15}	158 ± 19.74	4.8	5.8
10^{-14}	329 ± 20.87	1.7	3.8
10^{-13}	405 ± 12.15	3.9	2.9
10^{-12}	440 ± 13.2	9.3	2.7
10^{-11}	497 ± 14.91	1.64	2.6
10^{-10}	533 ± 13.99	1.6	2.1
10^{-9}	577 ± 17.31	8.19	1.9
10^{-8}	598 ± 16.2	9.12	1.6
10^{-7}	614 ± 12.42	10.3	1.3

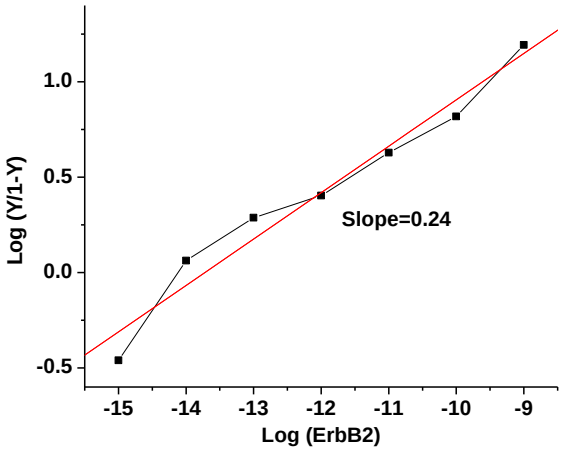

Figure S8. Hill plot showing $\log\frac{Y}{1-Y}$ as a function of log [*ErbB2*] where *Y* represents $\Delta R_{ct}/\Delta R_{ct\ (max)}$ and ΔR_{ct} represents change in charge transfer resistance.

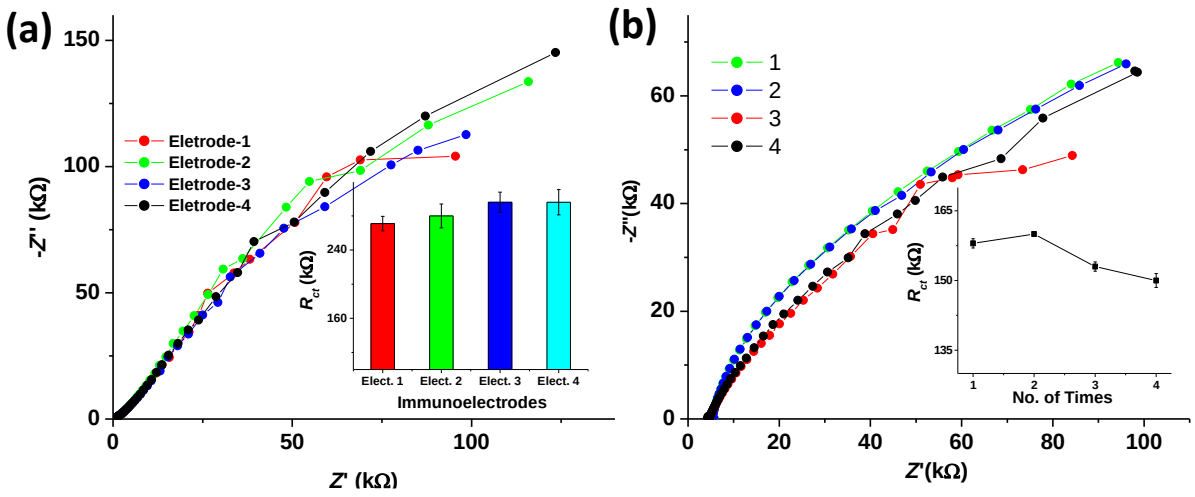

Figure S9. (a) Reproducibility test for four different immunoelectrodes (BSA/anti-ErbB2/GF-TiO_2) in presence of 10^{-14} M concentration of ErbB2 using impedance method. The inset shows R_{ct} versus number of immunoelectrodes. (b) Nyquist plots for four-time repeatability test of the fabricated immunosensor (BSA/anti-ErbB2/GF-TiO_2) at a 10^{-15} M concentration of ErbB2. The inset shows R_{ct} as a function of number of measurement times.